Studying Mutations in the Trm10 Methyltransferase to Reveal the Roles of Conserved Residues and Domains in Substrate Specificity and Catalytic Activity

A Senior Honors Thesis

Presented in partial fulfillment of the requirements for graduation *with honors research distinction* in Biochemistry in the undergraduate colleges of The Ohio State University

By

Tyler McClain

The Ohio State University

April 2021

Project Advisor: Dr. Jane E. Jackman, Department of Chemistry and Biochemistry

Abstract

tRNA modifications are a pivotal aspect of biology observed across all domains of life. These modifications rely on the presence of enzymes to induce the addition or deletion of groups on a tRNA. One of these enzymes is Trm10, which exists as three different homologs within the human body: denoted TRMT10A, TRMT10B, and TRMT10C. These proteins methylate at the N-1 position of nucleic acids at the 9th position of the tRNA, such that TRMT10A methylates a guanine to make N-1 methylguanosine (at the 9th position is denoted m^1G_9), TRMT10B methylates an adenine to make N-1 methyladenosine (at the 9th position is denoted m^1A_9), and TRMT10C performs both m^1G_9 and m^1A_9. In recent years, studies have demonstrated the importance of the SpoU Trm-D core of the protein (SPOUT core) in relation to this activity, but relatively little is known about the significant number of upstream and downstream residues on the protein, which comprise its N and C-terminal domains. These protein domains have little sequence conservation across species and domains of life, and their role in Trm10 activity remains unknown.

This project seeks to elucidate whether the presence of different upstream and downstream sequences would alter the activity of the SPOUT core of each type of TRMT10 by creating chimeric proteins where sequences from TRMT10A and B are mixed together. This way, terminal domains of TRMT10A are connected to a TRMT10B core and vice versa. Upon completion of this work, I have demonstrated that a construct with a TRMT10A core and TRMT10B upstream and downstream fragments (denoted BAB) does not show any activity, while all other TRMT10A core chimera retain m^1G_9 activity. On the other hand, no TRMT10B chimeric proteins displayed any activity in the assays I performed. These results suggest the

possibility that there is a role played in having at least one of the TRMT10A terminal domains present with the TRMT10A core, but this same phenomena does not exist with the TRMT10B core.

Introduction

It is well established that the flow of genetic information within organisms follows the central dogma of biology, with that being that genetic information DNA is transcribed into mRNA using RNA polymerases, which is then subsequently translated into protein via ribosomes with the help of tRNA. This simplified view overlooks multiple substages to this complex process, including regulatory steps. In all domains of life, this regulation exists through multiple different mechanisms, including through histone acetylation and deacetylation, mRNA alternative splicing, and tRNA modification, which is the most commonly modified RNA type (Phizicky and Hopper, 2010). These modification mechanisms along with their respective enzymes allow for the up and down regulation of translation, as well as alteration of tRNA activity as a whole (Jackman and Alfonzo, 2013). The enzymatic reactions which regulate tRNA activity include methylations, aminations, deaminations, thiolations, and many more complicated chemical changes (Jackman and Alfonzo, 2013). Many of these regulatory processes and their respective enzymes are conserved throughout most species, which suggests they may hold important roles in genetic information transfer (Swinehart et. al. 2013). With this being said, a major issue today in studying tRNA modification exists in the fact that the characterization of a post-transcriptional modification's effect on tRNA function is very complex, as it is quite common that multiple modifications work in conjunction with one another as well as the surrounding environment to alter the activity of the tRNA (Jackman and Alfonzo, 2013). Along with this, many unanswered questions exist for many of the tRNA modification enzymes where the molecular role of large portions of their amino acid sequences remain unknown, and Trm10 is no exception.

The tRNA methyltransferase 10, or Trm10, is one of the enzymes that methylates at the ninth position on a tRNA, and while its role in organisms at a large scale is unknown, it is still known to be important due to Trm10 being highly conserved across a plethora of Archaea and Eukarya, with most of the enzymes studied initially performing m^1G_9 activity (methylation of the guanosine at the 9th position), similar to the original enzyme in this family that was identified in the yeast *Saccharomyces cerevisiae* (Jackman et. Al., 2003; Swinehart et. Al., 2013; Van Laer et. Al., 2016). Some organisms encode more than one type of Trm10, with humans being one of those organisms along with other metazoa. There are 3 forms of human Trm10 homologs, which were named A, B and C (denoted *TRMT10A*, *TRMT10B*, and *TRMT10C*) (Vilardo et. al., 2020; Howell et. al. 2019). TRMT10A and TRMT10B are found in the cytosol, while TRMT10C is strictly a mitochondrial enzyme (Vilardo et. al., 2020; Howell et. al, 2019). It has been determined that TRMT10A performs m^1G_9 activity, while TRMT10B performs the m^1A_9 activity, and lastly TRMT10C performs both m^1G_9 and m^1A_9 activity within the mitochondria (Howell et. al., 2019; Vilardo et. Al., 2012). With this being said, $tRNA^{Asp}$ is the only known substrate for TRMT10B activity and it holds an adenine in the 9th position of the tRNA, while TRMT10A is less specific, and is capable of catalyzing m^1G_9 activity with many different tRNA substrates in vitro and in vivo (Howell et. al., 2019). It has recently been discovered that a lack of TRMT10A functionality in humans leads to microcephaly and metabolic defects, proving the essential nature of this enzyme in the body (Igoillo-Esteve et. al, 2013; Gillis et. Al., 2014). This also points to the independent nature of these proteins, as even in the presence of active TRMT10B or C (because the genes are unmutated in human patients who carry mutations in TRMT10A) these genetic diseases persist without TRMT10A functionality. While it is well established that the main active site for Trm10 tRNA modifications is the S-adenosyl methionine

(SAM) binding domain, there exists large N- and C-terminal domains on either side of the SAM binding domain that are largely unknown in regards to function (Krishnamohan and Jackman, 2017). In fact, studies have shown that the presence of the SPOUT core (SpoU-TrmD core) alone, which houses the SAM binding domain, is sufficient for each enzymes respective activity, but the presence and sequence conservation of parts of these seemingly extraneous sequences suggest they may be somewhat important. This SPOUT core shows high conservancy due to it housing the SAM binding domain. Being that these segments also compose a large portion of the protein by number of amino acids, it is important to determine their role, if any exists in regards to tRNA modification.

To better understand the function and roles that these N- and C-terminal segments play in TRMT10 activity, the DNA sequences corresponding to the TRMT10A and TRMT10B proteins were analyzed using a multi-species sequence alignment so that the conserved SPOUT sequences were not disrupted, and the sequences could be segmented without destroying the conserved residues (figure 1). In using this alignment-based approach, we aspired to create three segments from both human TRMT10A and TRMT10B followed by the splicing of segments from the different proteins to create new chimeric proteins composed of both TRMT10A and TRMT10B sequences. We named these new chimeric proteins by correlating the segments of each hybrid to their protein of origin using the letters A and B. For example, the BAA hybrid protein would be composed of the N-terminus fragment from the TRMT10B protein, the SPOUT core from TRMT10A, and the C-terminus fragment from TRMT10B. In total, six chimeric proteins were formed; three with TRMT10A cores, and three with TRMT10B cores (translated from assembled chimera in figure 2). In doing this, we sought to elucidate whether there was any effect that the N-terminal and C-terminal sequences held on the SPOUT core activity. Does there exist any

residues within the terminal domains that interfere with or promote catalysis? If so, are we able to determine if these exist within the N-terminal or C-terminal domain? The synthesis of these chimeric proteins was the first step to answering these questions in this thesis, and this was followed by the purification of the proteins and the subsequent testing for m^1G_9 and m^1A_9 activity using radioactive enzymatic activity assays (using substrates $tRNA^{Asp}$ to test m^1A_9 activity, and $tRNA^{trp}$ to test m^1G_9 activity). It was hypothesized that the protein's activity would be solely determined by whether a TRMT10A or a TRMT10B SPOUT core was present within the hybrid, as the SPOUT domain is where all conserved residues exist in these proteins.

Chapter 1: Cloning TRMT10A and TRMT10B Constructs to Generate Chimeric Proteins

To synthesize the TRMT10A and B chimeras, DNA synthesis for each fragment was required. Upon completing the analysis of wild type Trm10 amino acid sequences across multiple species, and determining conserved amino acids, break points in the wild type sequences were determined such that none of the conserved residues in the SPOUT catalytic core would be compromised by removal and replacement of the appended N- and C-terminal domains. This ensures that if these conserved residues hold catalytic function, this would not be destroyed in creating the chimeric proteins. Along with this, we decided to add an arbitrary sequence to the end of the C-terminal TRMT10B fragment, as this fragment based on the alignment and conserved residues was exceptionally short. This ensured that there was no loss of sequence during the assembly of the completed DNA vector later in the experiment. In total, five fragments of TRMT10A and five of TRMT10B were designed (figure 2). The five-fragment strategy was chosen to make it easier to assemble the gene for the complete chimeric protein from two fragments rather than to have to ligate each of the three domains (N-terminus, SPOUT core and C-terminus) independently. For example, to create the chimeric protein that is composed of an N-terminus TRMT10 A, a TRMT10A SPOUT core, and a TRMT10B C-terminus, we designed primers to amplify the two TRMT10A sections together as one fragment, while amplifying the TRMT10B C-terminus separately. Using the wild-type constructs for each protein as a template, primers for each fragment were designed, purchased, and used in conjunction with polymerase chain reaction (PCR) to synthesize these DNA fragments.

An agarose gel electrophoresis was performed to determine whether the size of the amplified fragments reflected the expected size. After confirming proper synthesis of the

individual fragments, the bands that matched the expected size were cut out to avoid contamination and unwanted sequences from being present in the assembly reactions. A gel extraction and PCR clean-up was performed to obtain the DNA fragment in solution and to minimize contaminants in the sample. Concentrations of each fragment were measured using a nanodrop instrument to ensure that sufficient amounts of each fragment were used in the assembly steps to follow. The fragments were then recombined and spliced together using Gibson assembly such that all possible hybrid sequences were formed. This type of assembly allows for precise "sticky ends" of certain length to be created on the double stranded DNA fragments using an exonuclease such that the single strand portion is complementary to that of another fragment with which it will be assembled to. Each of the five fragments were designed to generate appropriate sequences for assembly when performing the alignments of the wild type sequences in the first step. To ensure that the chimera sequences were assembled correctly and were ligated to the vector, the assembled reactions were then transformed into *Escherichia coli* cells and plated on LB plates containing ampicillin. This ensures that the only colonies that grow when incubated overnight are the ones that have the vector of focus, as the vector used in these experiments is designed to be resistant to ampicillin, conferring resistance into the *E. coli* within which it is transformed. With that being said, there still could be vectors transformed that do not contain the assembly, so minipreps were created for multiple colonies of each assembly. Agarose gels were then run for these minipreps following a restriction digest with specific restriction enzymes for the assemblies. This was used to visualize whether the properly assembled vector was created, because if it was the vector would be digested into appropriately sized bands on the agarose gel. To confirm this result, the samples that showed the expected patterns of digestion were sent for sequencing.

Results

Fragment Synthesis: The PCR performed to synthesize the fragments needed for this assembly appeared largely successful, with the initial round of fragment synthesis resulting in good yield for 9 out of the 10 fragments designed (figure 3). The sole exception to this was the fragment composed of the SPOUT core of TRMT10A and the C-terminus of TRMT10A (Fragment A2A3). This fragment was barely observable on the 1% agarose gel (figure 3, top gel), and the yield was so low that it was determined to be best to go through the PCR process once again with it. While doing this, we chose to perform a PCR screen testing alternative temperatures of annealing, substitution of buffers (using GC buffer designed for sequences with high guanine and cytosine content), and the inclusion of DMSO into the solution. Upon completing this PCR screen, the high temperature PCR procedure using the original mix for the PCR was found to yield the best results for the missing TRMT10A fragment (A2A3), so this sample was used moving forward. With the completion of this screen, we were able to obtain all of the fragments needed for the next steps.

Purification, Sequencing, and Quantification: The 10 fragments that appeared to be of the correct size were sequenced to confirm that they were correct. From there, each fragment was further purified using gel extraction and PCR clean up to remove contaminants before determining their concentrations using UV absorbance measured on a nanodrop instrument. Most fragment concentrations ranged from 0.05-0.07 μg/μL (figure 4). The two exceptions to this were the N-terminus and SPOUT core TRMT10B combined fragment (B1B2) and the C-terminus TRMT10B fragment (B3), which had concentrations of 0.0131 and 0.0146 μg/μL, respectively, which was somewhat low but judged to be still good enough to move forward with the next steps of the cloning process. Notably, due to the small size of the C-terminus

TRMT10B fragment (B3), the molar concentration of this fragment is correspondingly higher than it seems based on the mass concentration (μg/μL) and therefore was sufficient for assembly. Along with the concentrations obtained via nanodrop, the ratio of the absorbance values at 260 nm and at 280 nm were obtained for each of the fragments. This ratio allows for the purity of the DNA fragment to be assessed, as a pure sample of double-stranded DNA would be expected to exhibit a 260/280 value close to 1.80. For the most part, this was observed for each of the fragments, with the largest discrepancy being the N-terminal TRMT10B fragment at 1.50 (B1).

Gibson Assembly: With fragments assembled and their respective sequences confirmed, we were able to proceed with the Gibson Assembly of each chimeric sequence and into a prepared vector. When preparing the vector for assembly, it was important to linearize the DNA using a restriction enzyme so that the assembled gene sequence could be inserted into the vector. The prepared vector was digested and purified according to the procedure in the methods, yielding a final concentration of 0.0087 μg/μL with a 260/280 value of 1.80, so this vector was used for the assembly.

Using the concentrations for each amplified fragment obtained previously, it was important to ensure there was a specific mass of each fragment and vector added into the reaction mix. The first sequences to be assembled and transformed into cells to be plated onto LB+amp plates were the BAA, BBA, and AAB sequences (B1+A2A3, B1B2+A3, and A1A2+B3, respectively). It was observed that these transformations had rather low yields, with only a few colonies grown per plate. Nevertheless, two of each of these colonies were grown in liquid cultures for minipreps, which were eventually run on a 1% agarose gel upon being cut by the restriction enzymes PvuII (to indicate the presence of the TRMT10A core) and ClaI (to indicate the presence of the TRMT10B core). Subsequent assembly reactions with the other fragments

yielded many more colonies that were tested by restriction digest in the same way. Upon running all of the digested sequences on an agarose gel, it was determined that a successful vector assembly was obtained during the first round of assembly for the BAA, ABB, and BBA sequences, as these exhibited the correct digestion patterns on the gels. To ensure that this was the case, they were sent for sequencing which further confirmed these results. Generating the remaining constructs required additional colony screening and in two cases (AAB and BAB), also required additional assembly reactions to be carried out. After sequencing confirmed these results, expression constructs for all six protein chimera have been successfully created and we were ready to proceed to expression and purification for each of the chimeric proteins.

Chapter 2: Expression and Purification of Chimeric TRMT10A/TRMT10B Proteins

Upon obtaining the correctly assembled vectors for each of the chimeric TRMT10A/B sequences, the next step taken was to transform the DNA vector into BL-21 competent cells in preparation of growing cultures for these constructs. The BL-21 cells were utile in this situation due to the fact that these competent cells are exceptional for protein synthesis, and typically have a good protein yield when synthesizing proteins (Donahue and Bebee, 1999). Upon transforming the vector into these cells on an LB+Amp plate, 5 mL cultures were grown from the resulting colonies after incubation. The reason behind growing 5 mL cultures first lies in the fact that it is much easier to transfer a colony into a culture of small volume. From there, the 5 mL culture was sequentially transferred into a 25 mL culture and then to a 1 L culture upon visible growth. Throughout each of these steps, it was important to ensure that sufficient ampicillin was present in solution such that all other contaminating species that do not contain the ampicillin resistance that our vector provides would be killed off. To ensure sufficient and consistent growth across all cultures, the general protocol followed was to grow the 5 mL culture over the span of a day at 37ºC, then to grow the 25 mL culture (resulting from the transfer of the entire 5 mL of the previous culture) overnight at 37ºC before transferring sufficient volume of this culture into the 1 L culture such that the starting optical density (OD) taken at 600 nm is at 0.05. This allows for the growth time of this culture to be more predictable, as the doubling time for these cells is roughly 60 minutes, and the target optical density to achieve for induction with Isopropyl β-d-1-thiogalactopyranoside (IPTG) is OD_{600}~0.4-0.6.

Upon reaching the target OD_{600}, a sample of cells was taken and stored at -80ºC to use as a sample representing the proteins present prior to IPTG induction of the protein chimera (figure

5). From there, 1 mL of 1M IPTG was added to the culture and allowed to grow for 6 hours. These cultures were then able to be spun down, flash frozen using dry ice, and stored at -80ºC.

The next step was to purify the proteins that were obtained using metal affinity chromatography with TALON beads. The cobalt in the TALON beads binds to the 6-His tag engineered into the chimera proteins, allowing the remaining proteins synthesized during the process of culture growth to be eluted and removed throughout the multistep process of purification, ideally yielding the pure target protein. An important step in this process is the French Pressing of the cells such that they are lysed and the proteins are no longer held behind a plasma membrane, generating a crude soluble lysate. Upon completion of the washes that follow this stage and sequentially loading of the lysate onto the column, the protein was eluted off of the TALON beads by adding Imidazole. A high concentration of this molecule competes with the 6-His tag to bind with the TALON beads, effectively removing the protein from them. The eluted fractions were collected in multiple microcentrifuge tubes, and a 10 μL portion of each fraction was tested via Bradford Assay to determine the protein-containing fraction(s) by their blue color. This allowed me to determine which fractions contained the most concentrated proteins, and these fractions were pooled for further dialysis, where they would be concentrated and exchanged into an appropriate buffer for long-term storage. Our goal in this process is to get the most concentrated, pure protein, and all the steps discussed work towards this goal.

To analyze the results of this purification process, an SDS-PAGE experiment was run for each purified protein, analyzing the pure protein along with the washes performed during purification, the crude extract resulting from the lysis of the *E. coli* cells, the flow through (resulting solution after the introduction of TALON beads into the crude extract to bind the

target protein), and a ladder for size scaling (figure 5). This visualization allowed us to check the relative purity of the protein and to determine whether the protein is of the correct size.

Results

Upon completing this process for all six chimeric proteins, four (AAB, BAA, ABA, and BBA) were purified in relatively high yield and could be used directly in activity assays (see chapter 3). The BAB protein and the ABB protein did not appear to purify well the first time, as there was no clear and concise band present in the dialyzed fraction at the size expected for these proteins (see figure 5). Lack of pure ABB protein might be attributed to human error, as during this purification, the imidazole elution buffer, which removes the protein from the TALON beads, was added prematurely, and the protein was collected before the final wash and column elution procedure could be carried out (and thus required additional concentration).

Because the BAB protein was of the greatest concern, as we were not aware of any errors that occurred during its preparation, this protein was tended to first to determine optimal bacterial expression conditions for it.

The goal in running a test expression is to determine what conditions best suit the translation of the chimeric proteins we are interested in in the bacterial cells. In running this test expression the temperature at which the cells grow was tested along with the type of competent cells used, and the amount of IPTG used to induce target protein formation. All possible combinations of these conditions were studied, and upon being sonicated to induce the lysis of the cell, extracts corresponding to each condition were analyzed using SDS-PAGE (figure 6). The results between the ABA and the BAB proteins were consistent, as both SDS-PAGE gels

displayed that the use of Rosetta-pLysS cells at a growth temperature of 18ºC and 0.1 M IPTG were most beneficial for expression of both proteins. The only issue that arose regarded the BAB protein, as it was not the proper size according to the standards, which was noted, but it was still decided that these conditions would also be best for the other chimeric proteins. The rationale behind this decision is the fact that these proteins are translated from many similar mRNA sequences that are shared between multiple chimera, and therefore it was reasonable to assume that these expression conditions would apply to the rest of the chimera.

Unfortunately, when expressing and purifying the ABB chimeric protein using these optimized conditions, another issue arose, as it also appeared that the expressed protein was about 10 kD larger in size than expected according to the standards on the SDS-PAGE. At this point, it was decided to send the BAB miniprep in for sequencing to determine if this was a problem with the construct sequence. It was decided that sending the BAB fragment for sequencing would provide sufficient information regarding this issue, as both the BAB and ABB chimera displayed the same problem, allowing the assumption to be made that they were affected by the same issue. The results displayed the correct sequence, showing that this was not the issue. The isoelectric points of the proteins were also looked at, as a protein with a high isoelectric point may run aberrantly on an SDS gel. This was also not the issue, as both of the proteins experiencing issues had isoelectric points around 8-9, which is not outside of a typical range. At this point, its was assumed that we indeed had the right protein, but some unknown factor was affecting its ability to be resolved correctly on an SDS-PAGE experiment. Thus, at this point we had obtained all six of our chimeric proteins, although some questions remain about the status of the BAB and ABB proteins. The purified protein samples varied in concentration slightly, and ranged from less than 1 mg/mL to over 4 mg/mL in total concentration. Knowing

these concentrations will be important moving forward, as in order to perform activity assays, a certain amount of each protein must be present such that total amount of protein is equal across all samples.

Chapter 3: Activity Assays

For the final stage of this thesis, I used enzyme activity assays to determine whether the chimeric proteins synthesized in previous stages display m^1G_9 or m^1A_9 activity. In this process, we used alpha-ATP to uniformly label in vitro transcribed $tRNA^{Asp}$, as this tRNA has an adenine present at the ninth position (A_9), and is a known substrate for human TRMT10B. On the other hand, we use alpha-GTP to uniformly label an in vitro transcript of $tRNA^{Trp}$ to test for m^1G_9 activity, which is a known activity of humanTRMT10A. Uniform labeling is a process by which a tRNA is synthesized with three normal nucleotides and one radioactively labeled nucleotide, such that each position in the tRNA that corresponds to the labeled nucleotide is now replaced with the radioactive alternative. This labeling reaction is performed by T7 RNA polymerase using DNA templates that were created by a previous graduate student in the laboratory (Dr. Nathan Howell). This radiolabeled tRNA is useful in future procedures, as it facilitates imaging of the methylation activity of the chimera using thin layer chromatography (TLC), after a procedure described in more detail below. Imaging of each reaction will enable visualization of a radioactive spot on the TLC plate corresponding to the methylated nucleotide in the tRNA, which is separated from the unmethylated nucleotide because of its different mobility in the mobile phase of the chromatographic solvent.

Enzyme activity reactions were run in the presence of each chimeric enzyme and the labeled tRNA at 30ºC. Each enzyme was tested in three reactions, where the reaction was performed in subsequent ten-fold dilutions of enzyme concentration (undiluted, 1:10 dilution, 1:100 dilution). This allows for the visualization of the dependence of activity on the concentration of enzyme in each assay. It also allows for the inference of relative reaction rates, as an enzyme reacting at a high rate would still present a spot on a TLC plate, even if it is present

at a low concentration (while a less active enzyme might not generate a product spot at the lowest concentrations). The concentration of substrate tRNA added in each reaction was determined using the scintillation counter to measure the total radioactivity in the labeled preparation, and was approximately 3000 cpm/reaction.

Along with the chimeric proteins, this reaction was also performed with positive and negative controls to ensure the validity of the results. For m^1G_9 activity assays, both yeast Trm10 and WT human TRMT10A were used as positive controls, as they both are known to perform m^1G_9. For m^1A_9 assays, TkTrm10 was used as a positive control, as this enzyme has been shown to perform m^1A_9 (Singh et. Al., 2018, Krishnamohan et. Al, 2019). The negative control used was a reaction where no enzyme was present. These reactions were buffered and were performed in the presence of S-adenosyl methionine (SAM), as this acts as the methyl donor for the enzymes to act upon the substrate. Without SAM, the reactions would not be able to proceed. After one hour of reaction, the reactions were stopped by the addition of a large amount of a large amount of unlabeled yeast tRNA and a solution of phenol:chloroform, which completely denatures the protein and allows the RNA to be separated from the other reaction components. Then, a P1 nuclease was used to digest the tRNA into individual nucleotides, where they were visualized on a TLC plate. Without digestion, the tRNAs would run as a single spot on the TLC, making it impossible to determine whether methylation occurred or not.

Results

Upon completion of this process and the subsequent development of the TLC plates, imaging was performed, and these images were subsequently labeled and analyzed (figure 7).

All positive controls for both types of activity showed the appropriate patterns of methylation. In addition, the BAA and AAB constructs displayed m^1G_9 activity which tapered off in correspondence with the dilutions. It is important to note that the BAB construct did not perform m^1G_9, despite being expected to do so based on the results with BAA and AAB chimera. This expectation stemmed from the fact that this chimera still contains the TRMT10A SPOUT core, which typically would perform m^1G_9. There are several possible explanations for this phenomenon. First, this could occur due to the misfolding of the BAB protein causing inactivity in the protein, which did not occur when only one of the terminal domains was replaced. Another possibility could be the lack of robust expression that was observed in the BAB protein, which led to low purification yields and thus difficulty detecting activity. An exciting possibility lies in the idea that the C-terminal and N-terminal domains play a role in the enzymes activity, and in the situation when both of the domains have been replaced by sequences from TRMT10B, which are not normally associated with the SPOUT core, it is unable to perform it's activity. The determination as to which of these options is correct was unable to be made due to a lack of time for me to carry out more experiments, but is planned to be studied following the completion of this thesis.

From an m^1A_9 standpoint, there was no apparent activity in any of the tested chimera. Again, there are multiple factors that could contribute to this phenomenon. These factors mirror those which contributed to the issues with the BAB protein with regards to m^1G_9 activity. Along with those previously discussed, there is a possibility that the chimeras performed m^1A_9 activity at a much lower rate than that of TkTrm10, such that they were not visible on the assay conducted. Regardless, this assay suggests that the chimeras are affected by the alterations of the appended domains on the protein's SPOUT core. Moving forward, the chimera proteins will be

assayed at a higher concentration to determine if any activity can be detected under these conditions. Again, it is important to note that this assay was performed before the test expressions discussed previously, so the new protein purification resulting from the test expressions may alter the outcome of the assays in the future.

Overall, these assays show that the activity of the TRMT10A SPOUT domain is not fully dependent on having both C- and N-terminal TRMT10A domains appended to the SPOUT core. Initial data suggests that there does exist some level of dependence on having at least one of these fragments be TRMT10A, as the BAB construct does not show methylation. On the other hand, the complete loss of m^1A_9 activity for any of the tested chimera proteins suggests that there is some level of dependence on having TRMT10B C- and N-terminal fragments in the protein for catalytic activity. These are only preliminary results and are subject to change with future studies, but they give great insight into the importance of these appended domains on either side of the SPOUT domain.

Materials and Methods

PCR synthesis of fragments: Forward and reverse primers (2.5 μL of 10 μM concentration), template DNA (1 μL), dNTPs (1 μL of 10 μM concentration), 5x iProof buffer (10 μL), and iProof DNA polymerase (0.8 μL) were mixed in water (32.2 μL) to create a 50 μL solution before placing it in the thermal cycler to start the PCR process. It was ensured that no bubbles existed in the solution, and that all of the sample was at the bottom of the tube by spinning the sample before thermal cycling. The protocol for the thermal cycler can be broken down into four stages and was as follows: first stage: 98ºC for 1 min. Second stage: 98ºC for 30 s followed by 37ºC for 1 min and then 72ºC for 1 min (this cycle was repeated five times). Third stage: 98ºC for 30 s then 42ºC for 1 min followed by 72ºC for 1 min (this stage was repeated 25 times). Fourth stage: 72ºC for 10 min and then held at that temperature until removal from thermal cycler.

Vector Assembly: Using the gel purified and linearized vector resulting from digestion with *NruI* and *PmeI* (0.05 pmols used per reaction), the assembly solution was made along with the fragments needing to be assembled at a 1:10 dilution (such that 0.05 pmols of each fragment were introduced), and 10 μL of HiFi DNA master mix. These materials were placed in 10-*x* μL of water, where *x* corresponds to the total volume of fragments and vector in the solution. This was then incubated at 50ºC for 15 min, followed by transformation onto an LB+Amp plate. In this transformation, 2 μL of the previous reaction was mixed with 50 μL of NEB-5-α competent *E. coli* cells before plating the entire volume and incubating overnight at 37ºC.

Protein Prep: Protein preps for the chimeras were obtained using two protocols. The first used consisted of performing a transformation of the chimeric sequence of focus using BL-21 competent cells such that 50 μL of competent cells were mixed with 2 μL of the DNA. This

solution was iced for 30 min before being heat shocked at 50ºC for 45 s. Following this, the solution was iced for an additional 2 min before mixing with 300 μL of LB and plating 50 μL on an LB+amp plate to be incubated overnight at 37ºC. From there, colonies were selected and grown in 5 mL LB cultures with 5 μL of Ampicillin added. These were grown throughout a day before being transferred to 25 mL LB cultures with 25 μL of Ampicillin in the evening. These were grown overnight before the proper volume was transferred to a 1 L culture with 1 mL of ampicillin such that the starting OD_{600} was set at 0.05. This was grown until reaching an OD_{600} of roughly 0.5 before being induced with 1 mL of 1 mM IPTG and grown over the remainder of the day. All growth took place at 37ºC. These cultures were then spun down to form a pellet before being resuspended and transferred to two 50 mL conical vials. These vials were also spun for pelleting and flash frozen with dry ice before storing at -80ºC. The protocol differed following the test expressions performed, as multiple stages were changed. Firstly, the competent cells used in the transformation changed to Rosetta-Plyss. The remaining transformation protocol stayed consistent. The next difference stemmed from the concentration of IPTG used for induction, as this changed to 1 mL of 0.1 mM IPTG. The last change made was the temperature of growth after induction to 18ºC. All other temperatures were consistent, but this alteration resulted in growing the liter culture overnight before spinning it down.

SDS-PAGE: To start, the SDS resolving gel was made, with 2.5 mL of 40% Acrylamide, 2.5 mL of 1.5 M Tris pH 8.8, 0.1 mL of 10% SDS, 4.85 mL of water, 0.1 mL of 10% APS, and 0.01 mL of TEMED. This was poured into the plates and allowed to polymerize. Then, the stacking gel was made with 0.5 mL of 40% Acrylamide, 0.62 mL of 1 M Tris pH 6.8, 0.05 mL of 10% SDS, 3.82 mL of water, 0.025 mL of APS, and 0.005 mL of TEMED. This was poured to the top of the plates and allowed to polymerize with a comb in it. The samples were then prepared

to be run using 10 uL of SDS running dye and 2 uL of each sample. These mixtures were then heated at 95ºC for 10 min. They were then loaded into the gels and run at 130 V until the bands were close to the bottom of the gel.

Upon completion of the gel, it was stained with Coomassie blue stain over one hour before using destain on it. These gels were then imaged over a light source and analzyed.

Activity Assay: First, a common mix was made for all of the reactions. When broken down to the volume per reaction, this mix contained 0.5 μL of 1000 mM Tris pH 8, 0.15 μL of 100 mM $MgCl_2$, and 0.25 μL of 20 mM SAM. The substate tRNA volume added into the common mix is dependent on the concentration of the hot tRNA, which is determined through the use of the scintillation counter. Lastly, water is added so that the total volume of the mix for each reaction is 9 μL. This volume is then mixed with 1 μL of an enzyme. It is important to dilute the concentrations of the enzymes such that their concentrations match the least concentrated chimera. They are diluted using a dilution buffer stock composed of 20 μL of 1 M Tris pH 7.5, 10 μL of 50 mg/mL BSA, 1 μL of DTT, and 969 μL of water. Upon mixing the common mix with the enzyme, the reaction is set at 30ºC for one hour. Upon completion of this, stop reactions are introduced to stop the process of methylation. The mix for these stop reactions consists of 2 μL of yeast tRNA (10 mg/mL), 50 μL of 1 M Tris pH 8, and 38 μL of water. These volumes are for each reaction, such that 90 μL were added to the 10 μL reactions performed previously. A PCA clean-up was then performed using PLG tubes. The samples were placed in the PLG tubes before being shaken, spun down for 5 minutes, and removing the aqueous top layer to be placed in a new microcentrifuge tube. 200 μL of 100% ethanol was then added before placing them at -20ºC for 30 min. The tubes were then spun at 4ºC for 15 min before removing the 100% ethanol (ensuring that the pellet formed is not disturbed). 200 μL of 70%

ethanol was then added as a wash, where it was then spun down once again at 4ºC for 15 min. Once all ethanol was removed, the P1 digest mix was added. This consisted of 2.6 μL of 50 mM NaOAc (pH 5.2), 0.4 μL of 2 mM $ZnCl_2$, and 1 μL of 1 mg/mL P1 nuclease. These volumes are per reaction. The tRNA in solution was then digested at 50ºC for one hour before spotting 2 μL on a TLC plate and developing in a tank overnight. These results were then able to be imaged using a Typhoon.

Figures

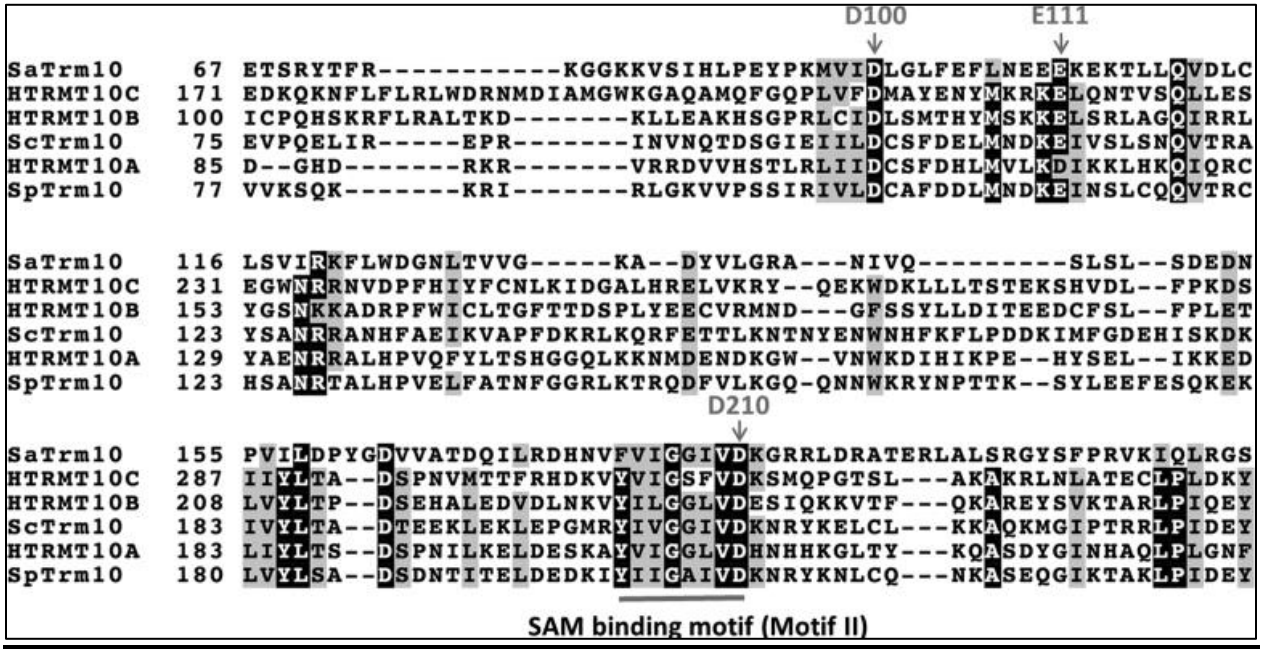

Figure 1: Sequence alignment. Conserved and potentially important sequences of Trm10 across multiple species**.** Include Human TRMT10A, B, and C, *S. cerevisiae* Trm10, *S. Acidocaldarius* Trm10, and *S. Pombe* Trm10.

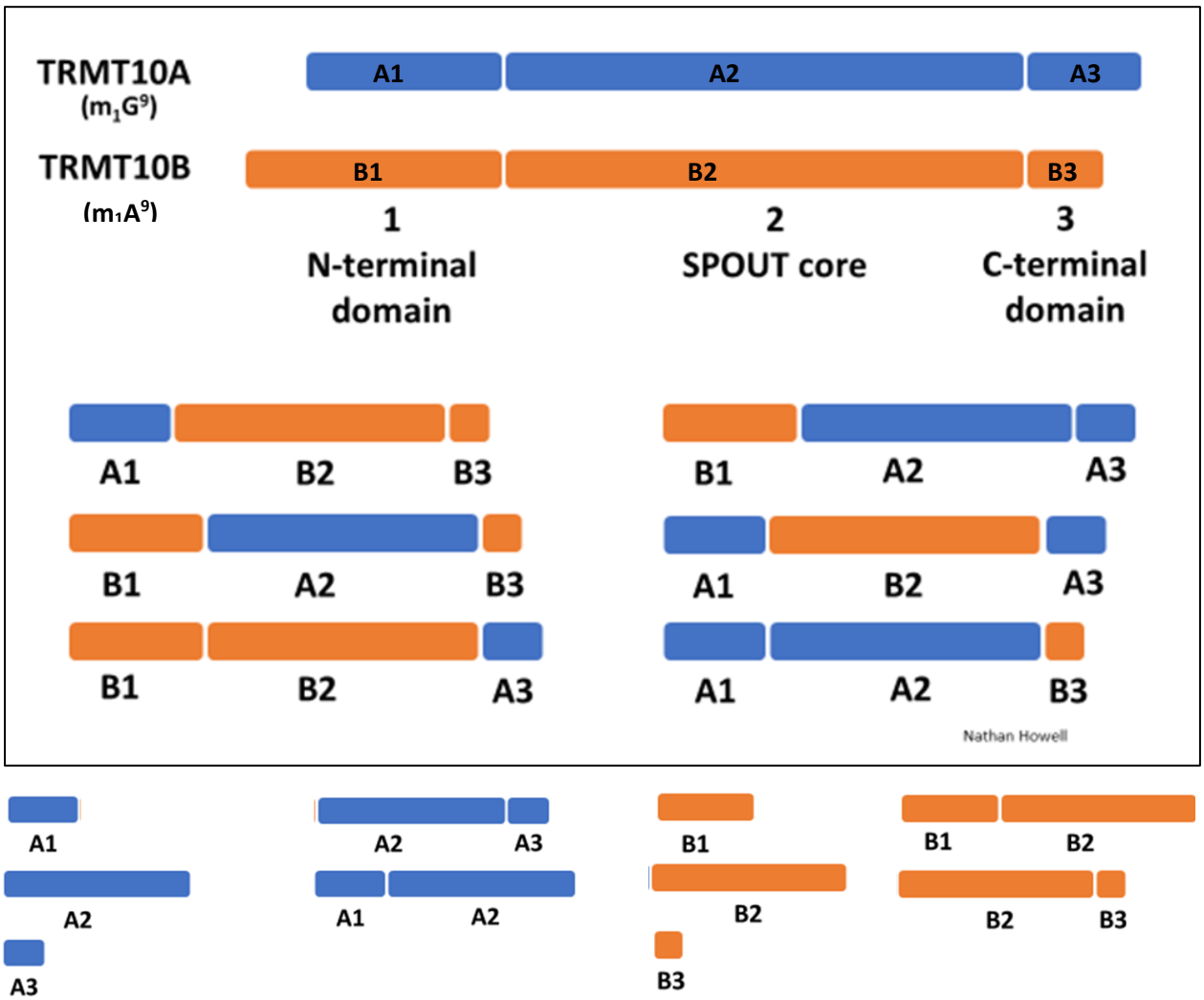

Figure 2: Chimeric Sequences of TRMT10. The wild type TRMT10A and B DNA was fragmented and spliced together to yield six different chimera DNA sequences (above). Fragments made to assemble these sequences seen at bottom. Adapted from figure made by Dr. Nathan Howell.

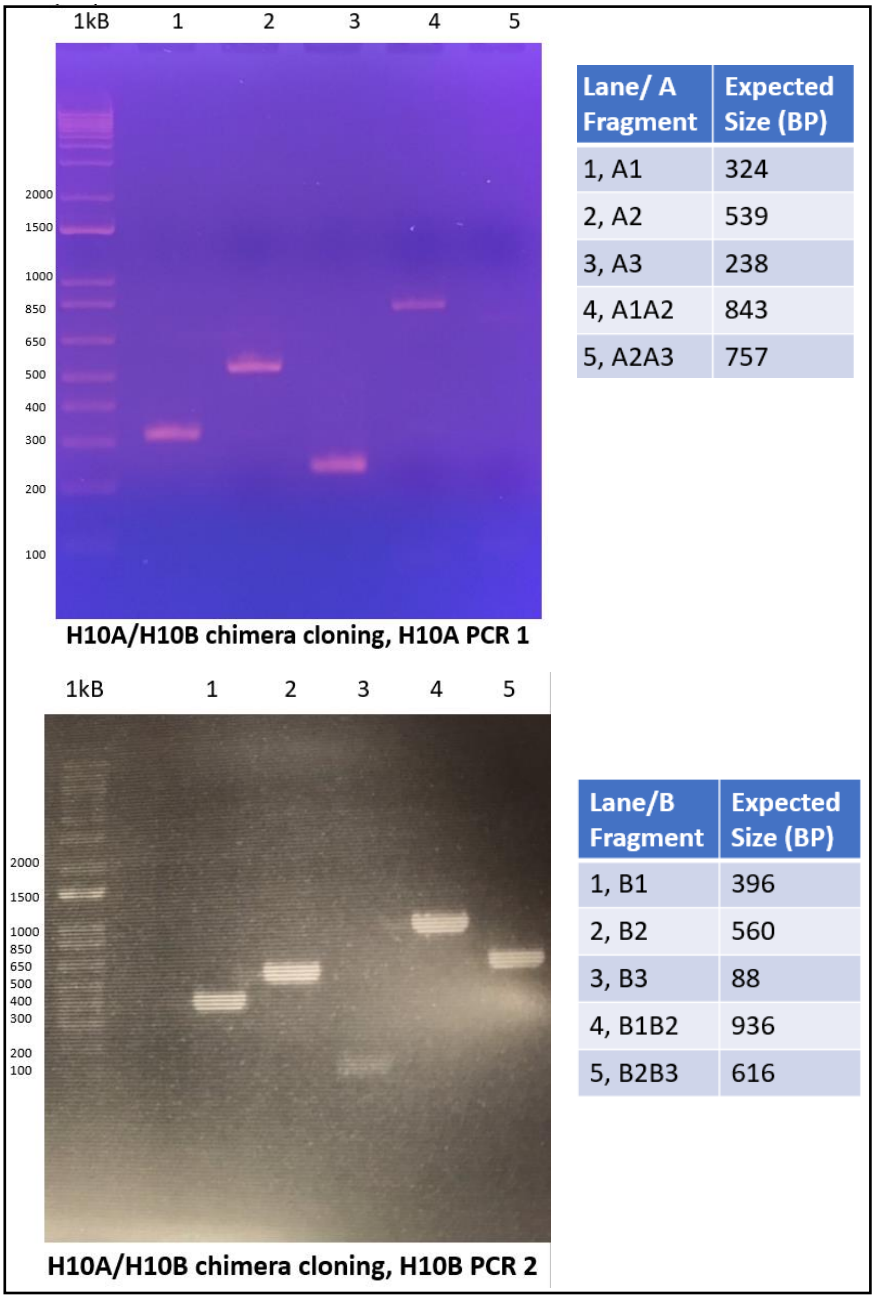

Lane/ A Fragment	Expected Size (BP)
1, A1	324
2, A2	539
3, A3	238
4, A1A2	843
5, A2A3	757

Lane/B Fragment	Expected Size (BP)
1, B1	396
2, B2	560
3, B3	88
4, B1B2	936
5, B2B3	616

Figure 3: Agarose gels for TRMT10A/B fragments. Display of the fragments and their respective sizes. Lane 5 in the first gel displays the only low product yield, which was corrected in later stages with a PCR screen.

Fragment Identity	Concentration (ug/uL)	260/280
A1	0.0481	1.85
A2	0.0642	1.86
A3	0.0660	1.84
A1A2	0.0131	1.85
A2A3	0.0653	1.80
B1	0.0925	1.50
B2	0.0937	1.84
B3	0.0146	1.87
B1B2	0.0780	1.84
B2B3	0.0657	1.90
Vector	0.0087	1.80

Figure 4: TRM10 Fragment and Vector Concentrations. Determined using nanodrop. Important for Gibson assembly. 260/280 value gives insight into purity of sample.

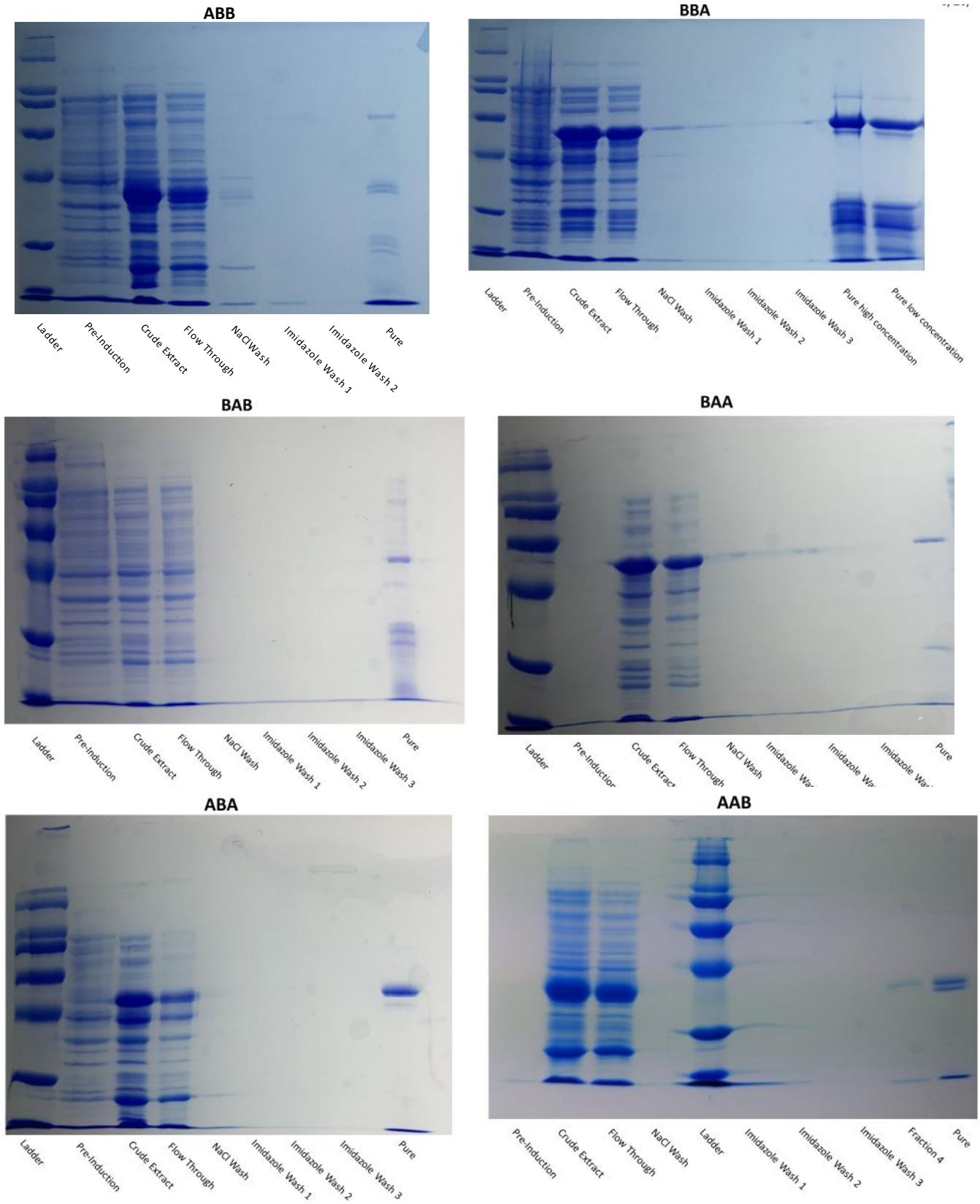

Figure 5: SDS-PAGE Analysis of Protein Expression. Gels run for each protein made. Lane identity displayed for each case.

BAB 37 C Rosetta

Wells (left to right)	Identity
1	Ladder
2	0 mM IPTG Crude Extract
3	0 mM IPTG Unlysed
4	0.1 mM IPTG Crude Extract
5	0.1 mM IPTG Unlysed
6	GAP
7	0.5 mM IPTG Crude Extract
8	0.5 mM IPTG Unlysed
9	1 mM IPTG Crude Extract
10	1 mM IPTG Unlysed

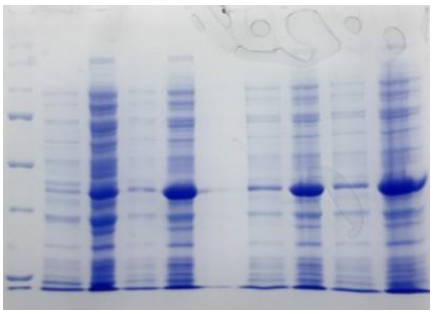

BAB 18 C Rosetta

Wells (left to right)	Identity
1	Ladder
2	0 mM IPTG Crude Extract
3	0 mM IPTG Unlysed
4	0.1 mM IPTG Crude Extract
5	0.1 mM IPTG Unlysed
6	0.5 mM IPTG Crude Extract
7	0.5 mM IPTG Unlysed
8	1 mM IPTG Crude Extract
9	1 mM IPTG Unlysed
10	GAP

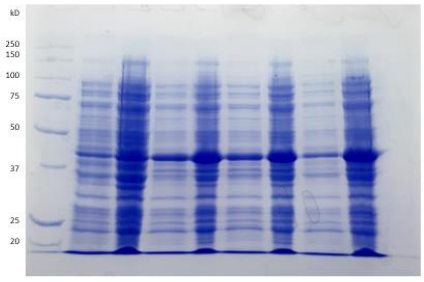

EXPECTED SIZE 35.15 kD

BAB 37 C BL-21

Wells (left to right)	Identity
1	Ladder
2	0 mM IPTG Crude Extract (well broke)
3	0 mM IPTG Crude Extract
4	0 mM IPTG Unlysed
5	0.1 mM IPTG Crude Extract
6	0.1 mM IPTG Unlysed
7	0.5 mM IPTG Crude Extract
8	0.5 mM IPTG Crude Extract (Well Broke)
9	0.5 mM IPTG Unlysed
10	1 mM IPTG crude extract
11	1 mM IPTG Unlysed

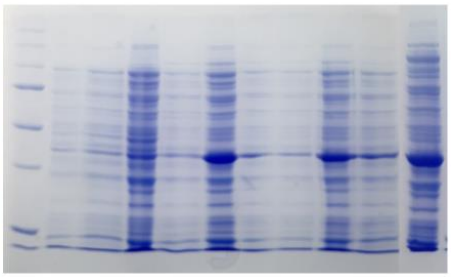

BAB 18 C BL-21

Wells (left to right)	Identity
1	Ladder
2	0 mM IPTG Crude Extract
3	0 mM IPTG Unlysed
4	0.1 mM IPTG Crude Extract
5	0.1 mM IPTG Unlysed
6	0.5 mM IPTG Crude Extract
7	0.5 mM IPTG Unlysed
8	1 mM IPTG Crude Extract
9	1 mM IPTG Unlysed
10	GAP

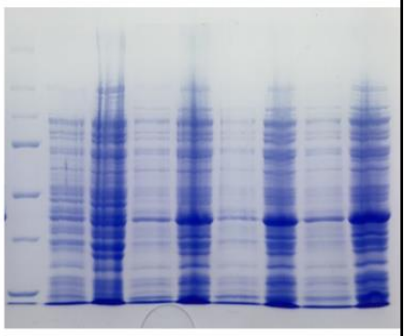

Figure 6A: BAB Expression Tests. Expression tests performed on the BAB construct altering temperature, competent cell choice, and IPTG concentration

ABA 37 C Rosetta

Wells (left to right)	Identity
1	Ladder
2	0 mM IPTG Crude Extract
3	0 mM IPTG Unlysed
4	0.1 mM IPTG Crude Extract
5	0.1 mM IPTG Unlysed
6	0.5 mM IPTG Crude Extract
7	0.5 mM IPTG Unlysed
8	1 mM IPTG Crude Extract
9	1 mM IPTG Unlysed
10	GAP

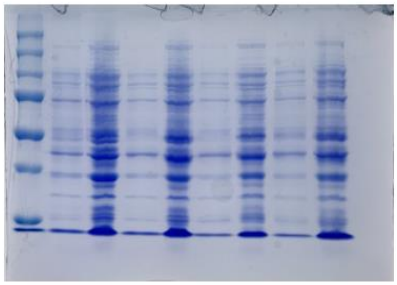

ABA 18 C Rosetta

Wells (left to right)	Identity
1	Ladder
2	GAP
3	0 mM IPTG Crude Extract
4	0 mM IPTG Unlysed
5	0.1 mM IPTG Crude Extract
6	0.1 mM IPTG Unlysed
7	0.5 mM IPTG Crude Extract
8	0.5 mM IPTG Unlysed
9	1 mM IPTG Crude Extract
10	1 mM IPTG Unlysed

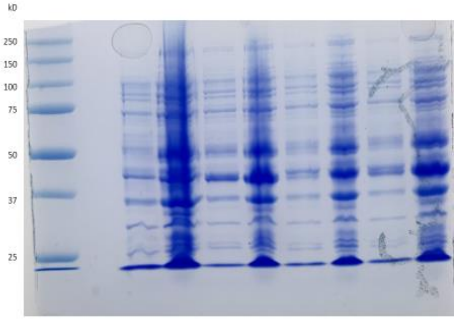

EXPECTED SIZE 40.19 kD

ABA 37 C BL 21

Wells (left to right)	Identity
1	0 mM IPTG Crude Extract
2	0 mM IPTG Unlysed
3	0.1 mM IPTG Crude Extract
4	0.1 mM IPTG Unlysed
5	Ladder
6	GAP
7	0.5 mM IPTG Crude Extract
8	0.5 mM IPTG Unlysed
9	1 mM IPTG Crude Extract
10	1 mM IPTG Unlysed

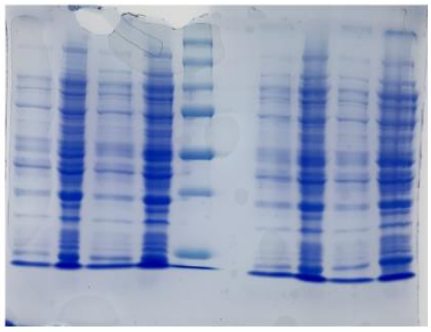

ABA 18 C BL 21

Wells (left to right)	Identity
1	Ladder
2	0 mM IPTG Crude Extract
3	0 mM IPTG Unlysed
4	0.1 mM IPTG Crude Extract
5	0.1 mM IPTG Unlysed
6	GAP
7	0.5 mM IPTG Crude Extract
8	0.5 mM IPTG Unlysed
9	1 mM IPTG Crude Extract
10	1 mM IPTG Unlysed

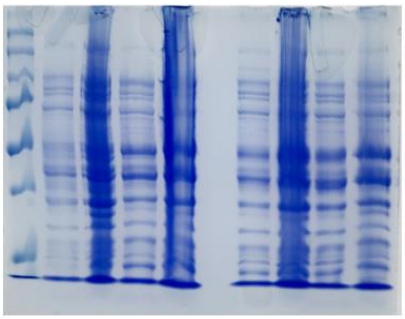

Figure 6B: ABA Expression Tests. Expression tests performed on the ABA construct altering temperature, competent cell choice, and IPTG concentration.

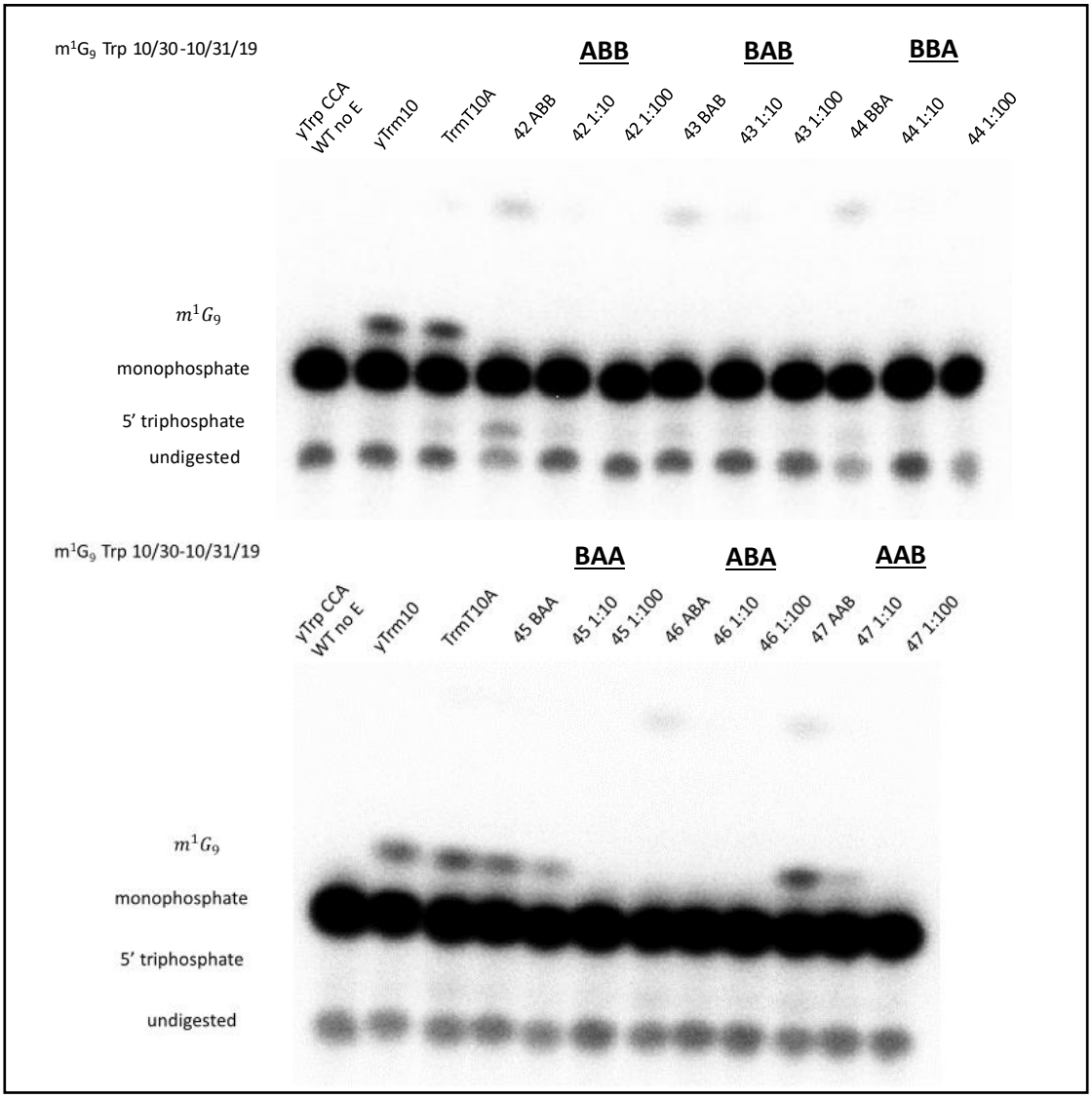

Figure 7A: m^1G_9 assays. Assays performed using chimeric enzymes and Trp tRNA. Images show that BAA and AAB chimera perform m^1G_9 activity.

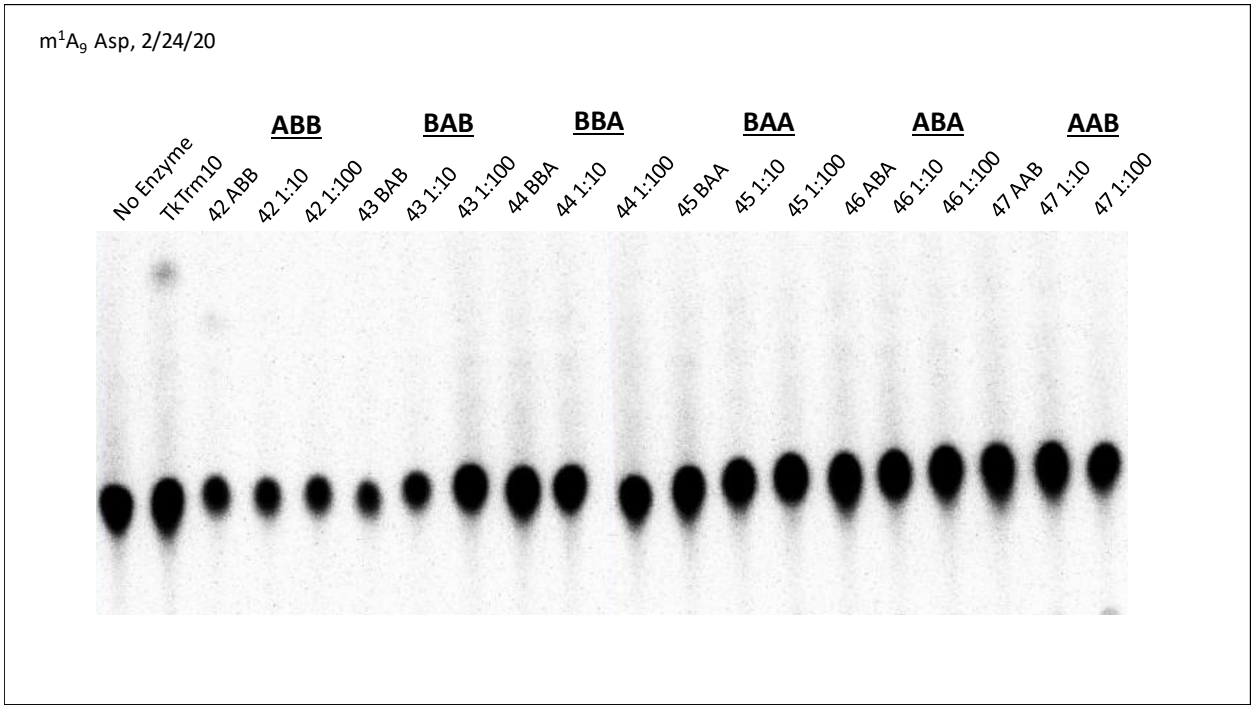

Figure 7B: m^1A_9 assays. Images show a lack of methylation for all protein chimeras, but the positive control was successful in methylation.

References

Donahue R, Bebee R. 1999. BL21-SI ™ Competent Cells for Protein Expression in E.coli. Org.in. [accessed 2021 Apr]. http://www.cdfd.org.in/pdfs/lbg/BL21-SIpaper.pdf.

Gillis D, Krishnamohan A, Yaacov B, Shaag A, Jackman JE, Elpeleg O. 2014. TRMT10A dysfunction is associated with abnormalities in glucose homeostasis, short stature and microcephaly. J Med Genet. 51(9):581–586.

Howell NW, Jora M, Jepson BF, Limbach PA, Jackman JE. 2019. Distinct substrate specificities of the human tRNA methyltransferases TRMT10A and TRMT10B. RNA. 25(10):1366–1376.

Igoillo-Esteve M, Genin A, Lambert N, Désir J, Pirson I, Abdulkarim B, Simonis N, Drielsma A, Marselli L, Marchetti P, et al. 2013. tRNA methyltransferase homolog gene TRMT10A mutation in young onset diabetes and primary microcephaly in humans. PLoS Genet. 9(10):e1003888.

Jackman JE, Alfonzo JD. 2013. Transfer RNA modifications: nature's combinatorial chemistry playground: Transfer RNA modifications. Wiley Interdiscip Rev RNA. 4(1):35–48.

Jackman JE, Montange RK, Malik HS, Phizicky EM. 2003. Identification of the yeast gene encoding the tRNA m1G methyltransferase responsible for modification at position 9. RNA. 9(5):574–585.

Krishnamohan A, Dodbele S, Jackman JE. 2019. Insights into catalytic and tRNA recognition mechanism of the dual-specific tRNA methyltransferase from Thermococcus kodakarensis. Genes (Basel). 10(2):100.

Krishnamohan A, Jackman JE. 2017. Mechanistic features of the atypical tRNA m1G9 SPOUT methyltransferase, Trm10. Nucleic Acids Res. 45(15):9019–9029.

Phizicky EM, Hopper AK. 2010. tRNA biology charges to the front. Genes Dev. 24(17):1832–1860.

Singh RK, Feller A, Roovers M, Van Elder D, Wauters L, Droogmans L, Versées W. 2018. Structural and biochemical analysis of the dual-specificity Trm10 enzyme from Thermococcus kodakaraensis prompts reconsideration of its catalytic mechanism. RNA. 24(8):1080–1092.

Van Laer B, Roovers M, Wauters L, Kasprzak JM, Dyzma M, Deyaert E, Kumar Singh R, Feller A, Bujnicki JM, Droogmans L, et al. 2016. Structural and functional insights into tRNA binding and adenosine N1-methylation by an archaeal Trm10 homologue. Nucleic Acids Res. 44(2):940–953.

Vilardo E, Amman F, Toth U, Kotter A, Helm M, Rossmanith W. 2020. Functional characterization of the human tRNA methyltransferases TRMT10A and TRMT10B. Nucleic Acids Res. 48(11):6157–6169.

Vilardo E, Nachbagauer C, Buzet A, Taschner A, Holzmann J, Rossmanith W. 2012. A subcomplex of human mitochondrial RNase P is a bifunctional methyltransferase--extensive moonlighting in mitochondrial tRNA biogenesis. Nucleic Acids Res. 40(22):11583–11593.

William E. Swinehart, Jeremy C. Henderson, Jane E. Jackman. 2013 Jun 23. Unexpected expansion of tRNA substrate recognition by the yeast m1 G9 methyltransferase Trm10. Cshlp.org. [accessed 2021 Apr 13]. https://rnajournal.cshlp.org/content/19/8/1137.full.pdf+html.